Time-resolved Mueller matrix imaging polarimetry

Ihor Berezhnyy and Aristide Dogariu

College of Optics and Photonics,
University of Central Florida, Orlando, FL 32816-2700

Abstract: We present a new method of time-resolved Mueller matrix imaging polarimetry for spatial and temporal characterization of the polarization effects in backscattering from turbid media. The technique allows measuring the time evolution of spatially varying polarization patterns of diffusely backscattered light with picosecond resolution. A series of time-resolved polarization patterns are obtained at various time delays, are analyzed in sequence, and used to separate the polarimetric contributions of different scattering paths. Specific features of the 2D Mueller matrix components corresponding to light backscattered from colloidal suspensions were determined and characterized. The temporally- and spatially-resolved measurements permit detailed analysis of the changes in the magnitude, sign, and the general symmetry properties of Mueller matrix components.

References and links

1. J. Cariou, B. Le Jeune, J. Lotrian, Y. Guern, "Polarization effects of seawater and underwater targets," Appl. Opt. **29**, 1689-1695 (1990).
2. B.Kaplan, G. Ledanois, B. Villon, "Mueller Matrix of Dense Polystyrene Latex Sphere Suspensions: Measurements and Monte Carlo Simulation," Appl. Opt. **40**, 2769-2777 (2001).
3. A. Dogariu, C. Kutsche, P. Likamwa, G. Boreman, B. Moudgil, " Time-domain depolarization of waves retroreflected from dense colloidal media," Opt. Lett. **22**, 585-587 (1997).
4. S. G. Demos, R. R. Alfano, "Optical polarization imaging," Appl. Opt. **36**, 150-155 (1997).
5. J. R. Mourant, T. M. Johnson, J. P. Freyer, "Characterizing Mammalian Cells and Cell Phantoms by Polarized Backscattering Fiber-Optic Measurements," Appl. Opt. **40**, 5114-5123 (2001).
6. W.S. Bickel, W.M. Bailey, "Stokes vectors, Mueller matrices, and polarized scattered light," Am. J. Phys. **53**, 468-478 (1985).
7. W. S. Bickel, A.J. Watkins, and G.Videen, "The light-scattering Mueller matrix elements for Rayleigh, Rayleigh–Gans, and Mie spheres," Am. J. Phys. **55**, 559-561 (1987).
8. A. H. Heilscher, A. A. Eick, J. R. Mourant, D. Shen, J. P. Freyer, I. J. Bigio, "Diffuse backscattering Mueller matrices of highly scattering media," Opt. Express **1**, 441-453 (1997).
9. G. Yao, L. Wang, "Propagation of polarizes light in turbid media: simulated animation sequences," Optics Express **7**, 198-203 (2000).
10. M. J. Racovic, G. W. Kattawar, M. Mehrubeoglu, B. D. Cameron, L. V. Wang, S. Rastegar, G. L. Cote, "Light backscattering polarization patterns from turbid media: theory and experiment," Appl. Opt. **38**, 3399-3408 (1999).
11. H. C. Van de Hulst. *Light Scattering by Small Particles*. (John Wiley & Sons, NewYork, NY, 1957), 47.
12. R. M. A. Azzam, "Photopolarimetric measurement of the Mueller matrix by Fourier analysis of a single detected signal," Opt. Lett. **2**, 148-150 (1978).

1. Introduction

At present, the unrelenting research involving light propagation and scattering in turbid media is noticeably focused on studies of diffusely backscattered light. By sending a polarized laser beam onto a sample and by subsequently measuring and analyzing the state of polarization of

scattered light, it is possible to obtain information about a variety of physical parameters which characterize a scattering medium or a distant object. This methodology has vast applications including remote sensing, underwater imaging, and determination of the average photon path length [1-3]. A particularly strong interest in understanding the properties of diffusely backscattered light has emerged in biomedical studies [4, 5]. Furthermore, the measurement of polarization parameters of the light scattered in the backward direction benefits from a relatively simple, fast, and convenient data acquisition procedure, which motivates the ongoing efforts aimed at further developing the backscattering polarization imaging technology.

A comprehensive understanding of light propagation and scattering for the most general case of highly scattering media is yet to be attained. An analysis based on the Stokes vector - Mueller matrix approach provides a theoretical framework, which can be directly related to the experimentally measurable parameters [6,7]. Recently, the Stokes vector - Mueller matrix approach for scattering has been extended to characterization of spatially varying polarization patterns for diffusely backscattered light [8]. In this approach, determining 16 components of the Mueller matrix for the studied object gives a comprehensive description of scattering properties of a sample or a medium in the spatial domain. Rather then being just one number, each of the 16 components of the Mueller matrix is, in fact, a two-dimensional (2D) array of numbers, corresponding to different spatial locations across the surface of the object or medium.

Another aspect of backscattering from diffuse media is the temporal evolution. In this work, we demonstrate new capabilities for studying diffusely backscattered light by presenting, for the first time, experimental results for simultaneously recorded time-resolved and spatially-resolved Mueller matrices. As the intensity patterns for diffusely backscattered light vary not only in space, but also in time, our data allows a complete spatial-temporal description of vector properties of a multiple scattering process.

The paper is organized as follows. First, the operational principles of the experimental procedure are described. Then, the experimental section presents results of time-resolved measurements of 2D Mueller matrix obtained in backscattering from dense colloidal media. Next, we discuss the symmetry properties of the measured Mueller matrix components and we clarify some contradictions existing between theoretical, numerical, and experimental works concerned with Mueller matrices for diffusive media. The conclusion section points out the overall significance of the novel experimental approach and discusses the prospects for information retrieval.

2. Concept of backscattering Mueller matrix

In general, light interaction with a medium changes its polarization state. Therefore, by analyzing the polarization state of an optical field after it passes through or is scattered from a random medium, one can retrieve information about properties of that medium. In the Stokes vector-Mueller matrix approach, a polarization state of light is represented by a four-component Stokes vector and, consequently, light interaction with the medium is described by a 4x4 matrix. This sixteen-component matrix, which is known as the Mueller or scattering Mueller matrix (if scattering is involved) fully characterizes the scattering polarization phenomena caused by light interaction with a turbid medium. Knowledge of the Mueller matrix for the medium permits calculating the polarization state of the scattered light for any given polarization state of the probing beam. On the other hand, the Mueller matrix is determined by properties of the scattering medium, which allows determining various characteristics of the medium such as an average size of the scattering particles, particle shape, scatterer spatial distribution, refractive index of the medium, scattering coefficient and anisotropy factor, etc. In addition, one can analyze different physical aspects of the scattering process; for example, one can understand how the coherence properties of light fields are modified as a result of scattering. Therefore, determination of the Mueller matrix of the scattering object is the major goal in studies of light scattering phenomena.

Theoretically, the Mueller matrix of a scattering medium can be obtained by solving the Maxwell's equations with the corresponding boundary conditions. This requires stipulating the appropriate assumptions concerning the scattering process as well as the properties of the medium and involves intense numerical calculations. Solving directly the Maxwell's equations for the general case of multiple scattering media appears to be a computationally unrealistic task and the problem is usually approached using the Monte Carlo technique for simulation of polarization-dependent photon propagation through the scattering media [9].

Experimentally, the determination of the Mueller matrix is based on the measurement of the polarization states of the scattered light for the specified polarization state of the incident light, and subsequent calculation of the corresponding Mueller matrix components. Several modifications of the experimental methodologies for steady state measurement of the Mueller matrix were developed and applied to measurement of backscattered polarization patterns for different turbid media [8, 10].

As already noted, the properties of the Mueller matrix are dictated by the properties of the scattering medium. In the most general case, all 16 components M_{ij} of the Mueller matrix are independent [11]. However, depending on particular optical properties of the scattering object and the specificity of the scattering process, the number of independent components might be reduced due to symmetry relations or some components may completely vanish. A simple example is provided by the case of spherical scatterers where the symmetry properties of backscattering Mueller matrix vary depending on the scattering conditions. Specifically, the extreme cases of single scattering and fully randomized multiple scattering are rather well understood. However, the intermediate, sub-diffusing regimes are less studied and, at present, no consensus exists in the literature regarding the symmetry properties of Mueller matrix for this type of scattering conditions. To the best of our knowledge only steady state studies have been approached in this context. We performed a thorough analysis of the available computational and experimental data and found that the backscattering Mueller matrices obtained by different groups for this type of scattering process are contradictory with respect to the symmetry relations for the matrix components [8, 10]. For instance, according to Ref. [8], the Mueller matrix is symmetric: $M_{mn} = M_{nm}$. However, in Ref. [10] only three pairs of the off-diagonal components are symmetric: $M_{10} = M_{01}$, $M_{30} = M_{03}$, $M_{31} = M_{13}$. The rest of the off-diagonal components obey anti-symmetric relations $M_{20} = -M_{02}$, $M_{21} = -M_{12}$, $M_{32} = -M_{23}$ according to the data in Ref. [10]. The symmetry of the Mueller matrix reflects a fundamental characteristic of its internal structure which, in turn, is dictated by the properties of the scattering media; it should therefore be independent on the technique used to determine the matrix. Because complete information about deterministic and non-deterministic scattering systems can be obtained from the properties of the Mueller matrix, understanding these symmetry relations requires a more careful investigation.

3. Time-resolved imaging of backscattering Mueller matrix

Intensity patterns for the steady state backscattering Mueller matrix are formed as a result of mixing different orders of scattering. The particular fraction of each type of scattered photons depends on the properties of the scattering medium, as characterized by the reduced scattered coefficient. The major drawback of steady-state measurements is that it is not possible to separate the contribution to polarized light patterns due to single- scattered photons, from the randomized polarization patterns, emerging due to multiple scattering events. As a result, steady-state measurements can not determine the individual backscattering Mueller matrix corresponding to specific orders of scattering. The problem can only be approached by time-resolved imaging methods, such as the one we present here. The experimental technique allows tracing the backscattering Mueller matrix starting from the early stages of single scattering events until the outcoming light becomes fully unpolarized due to numerous scattering events.

3.1. Experimental setup

The experimental setup for picosecond time-resolved imaging Mueller matrix polarimetry in backscattered light geometry is shown schematically in Fig. 1. A pulsed Ti: sapphire laser (Tsunami, Model 3955, Spectra-Physics) is used to provide vertically polarized (ratio 1:500) pulsed light with ~130-fs pulses at 76-MHz repetition rate. The laser wavelength used here is 806 nm and the laser spot size is less than 2 mm. The beam passes through a rotating quarter wave-plate and impinges on the sample in an oblique direction. The scattered light which emerges from the sample is collected close to the backscattering direction at about 20 degree angle with respect to the probing light. The scattered light passes through a second rotating quarter wave-plate and an analyzing polarizer, and is then recorded by the picosecond ultra-fast gated intensified camera system (PicoStar, LaVision), afterward called CCD. The CCD resolution is 12 bit, it has an electronic time gate of 200 ps and a gating that can be varied with a time step of 25 ps. In this experiment, the specular reflection triggeres the CCD acquisition. The scattering suspension is placed in a rectangular thin-walled vessel. The surface with dimensions of 22.9x22.9 mm^2 is imaged into the frame, corresponding to 224x224 pixels (Fig. 2).
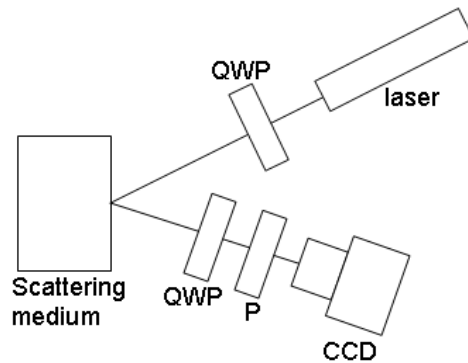
Fig. 1. Schematic of experimental setup: QWP - rotating quarter wave plate, P - static polarizer, CCD - ultra-fast gated intensified camera system.
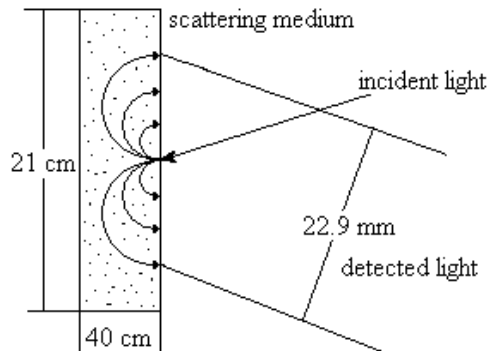
Fig. 2. Schematic of the geometry used in the experiment.

3.2 Principle of operation

The measurement technique is based upon an operational principle, which involves the modulation of a polarization state for both probing and out coming light beams as suggested earlier [12]. The resulting modulated light signal is collected by the CCD and is analyzed pixel by pixel to calculate individual intensity patterns, which correspond respectively to the 16 components of the backscattering Mueller matrix. In brief, the two quarter-wave plates, inserted in the probing and analyzing beam paths, are synchronously rotated with the ratio 1:5 to generate a periodic signal, which includes 12 harmonic terms and a dc term. This signal carries information about the properties of the medium which induces the transformation of the polarization state of the modulated probing light. The final complex signal is analyzed by a discrete Fourier transform algorithm to retrieve the information on the scattering object. We then calculate each of the 16 Mueller matrix components, which in this specific case are not single numbers, but two-dimensional data arrays, otherwise known as polarization patterns. The experimental procedure requires collecting of 48 intensity images at various orientations of the two quarter-wave plates. The described procedure provides the possibility to calculate the backscattering Mueller matrix for a given time step. It is then repeated for each time step in the desired time-series, thereby giving a time-resolved data set. In our measurements, we used 31 time steps in each of the time-series, which corresponds to acquiring a total of 31x48=1488 images. The entire procedure is fully automated.

3.3. Materials

Aqueous suspensions of monodisperse silica spheres with 200-nm and 1500-nm diameter were prepared at different concentrations. The reduced scattering coefficient μ_s' of the suspensions was, respectively, 0.03, 0.06, 0.12, 0.25, 0.32 cm^{-1} for the 200-nm particles and 0.32 cm^{-1} for the 1500-nm particles. The large dimensions of the container allowed us to consider the sample as a semi-infinite medium. To reduce the effect of tank surface scattering, the experimental procedure was first performed for the container filled with pure water, without scattering particles. The first series of images constitute an optical background and were subtracted from further measurements for the container. After that, the resulting data set was processed according to the algorithm as described above.

4. Results and discussion

Figures 3-7 illustrates several time frames of the time series for all 16 components of the backscattering Mueller matrix corresponding to a suspension of silica spheres with particle size 200 nm and Figs. 8-10 – for particle size of 1500 nm.
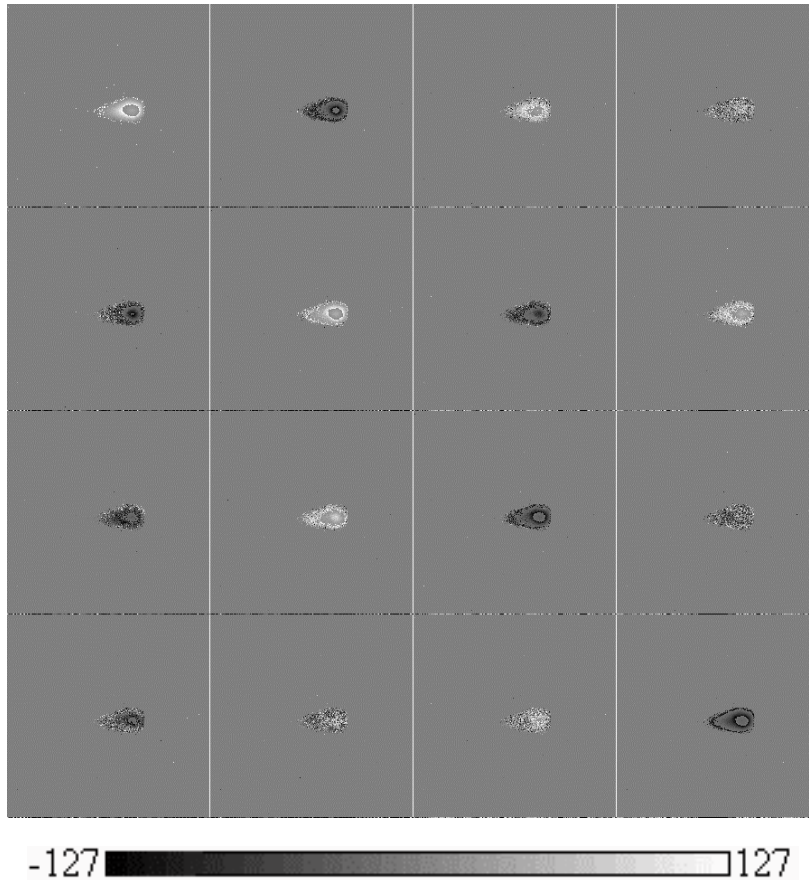
Fig. 3. Diffuse backscattering Mueller matrix components corresponding to a suspension of randomly distributed silica spheres (diameter 200 nm) with $\mu_s^{'} = 0.32\ cm^{-1}$. The gray scale bar is adjusted so that black corresponds to negative and white represents positive values of the matrix component. Gray color means "no light" or component change by an order of magnitude. Gate delay time is 100 ps.

In both cases, the scattering coefficient was at $\mu_s^{'} = 0.32\ cm^{-1}$. For the 200 nm particles, the corresponding patterns are presented at 100, 200, 325, 425 ps time delays respectively and at delays of 650, 950 ps for 1500 nm particles. For better visualization, we did not apply a normalization procedure to the matrix components. Figures 7, 10 represent the steady state Mueller matrix obtained by adding the separate time-resolved patterns for 31 subsequent time frames. The gray scale data bar is provided for each image with white and black corresponding to the positive and negative signs, respectively.
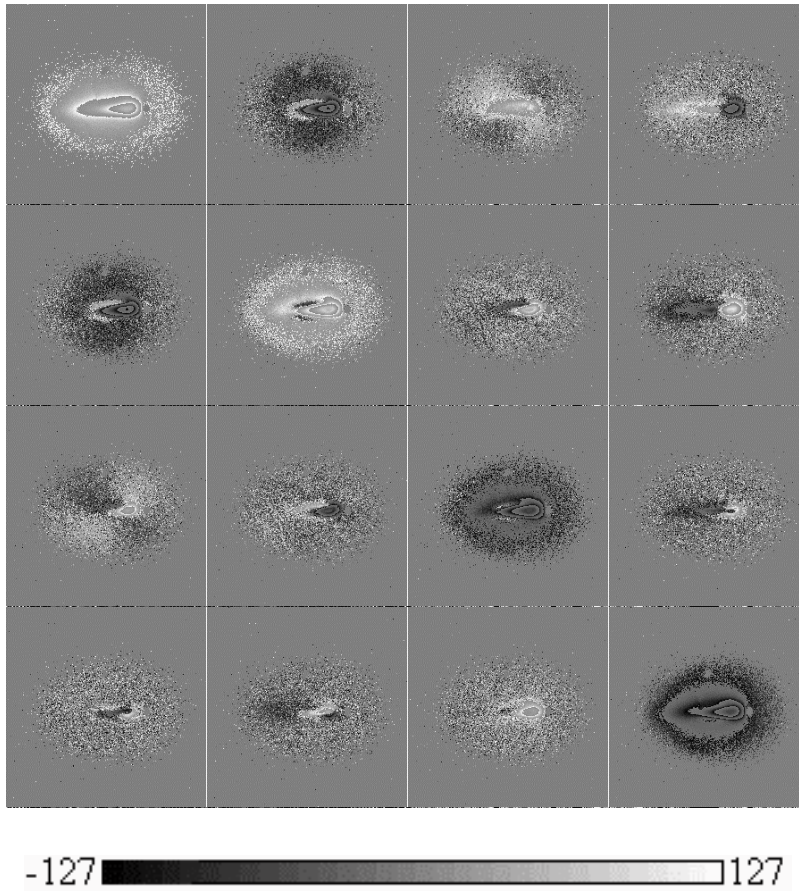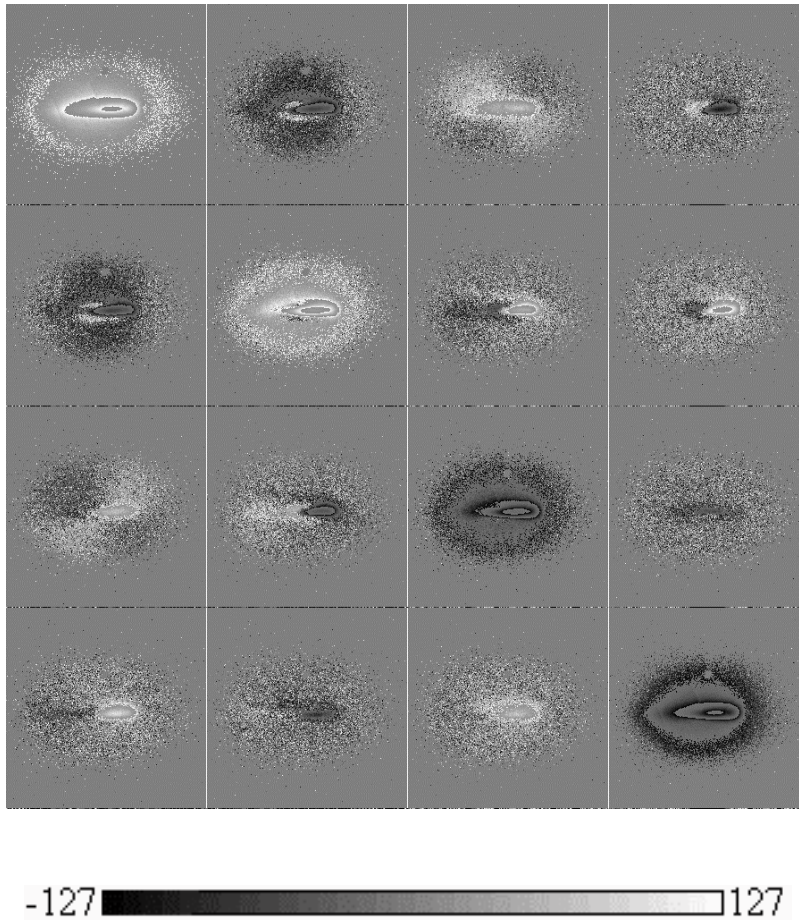
Fig. 4. Diffuse backscattering Mueller matrix components corresponding to a suspension of randomly distributed silica spheres (diameter 200 nm) with $\mu_s' = 0.32 \ cm^{-1}$. The gray scale bar is adjusted so that black corresponds to negative and white represents positive values of the matrix component. Gray color means "no light" or component change by an order of magnitude. Gate delay time is 200 ps.
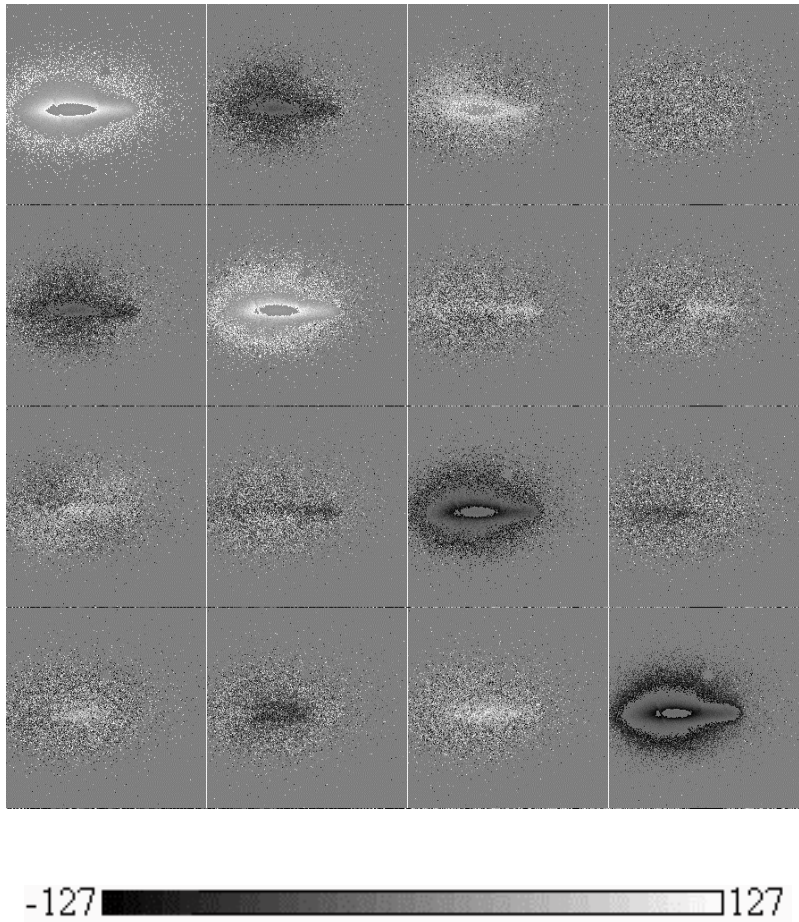
Fig. 5. Diffuse backscattering Mueller matrix components corresponding to a suspension of randomly distributed silica spheres (diameter 200 nm) with $\mu_s' = 0.32\ cm^{-1}$. The gray scale bar is adjusted so that black corresponds to negative and white represents positive values of the matrix component. Gray color means "no light" or component change by an order of magnitude. Gate delay time is 325 ps.

Fig. 6. Diffuse backscattering Mueller matrix components corresponding to a suspension of randomly distributed silica spheres (diameter 200 nm) with $\mu_s^{'} = 0.32 \ cm^{-1}$. The gray scale bar is adjusted so that black corresponds to negative and white represents positive values of the matrix component. Gray color means "no light" or component change by an order of magnitude. Gate delay time is 425 ps.
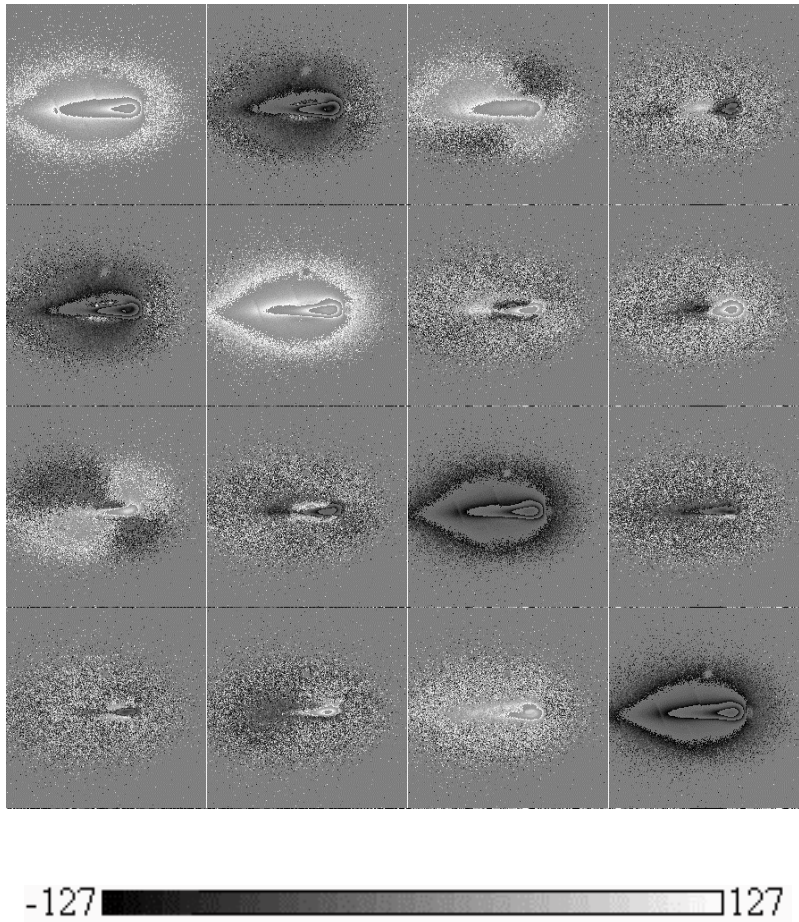
.

Fig. 7. Diffuse backscattering Mueller matrix components corresponding to a suspension of randomly distributed silica spheres (diameter 200 nm) with $\mu_s^{'} = 0.32 \ cm^{-1}$. The gray scale bar is adjusted so that black corresponds to negative and white represents positive values of the matrix component. Gray color means "no light" or component change by an order of magnitude. Time integrated matrix (integration for 31 time-steps).
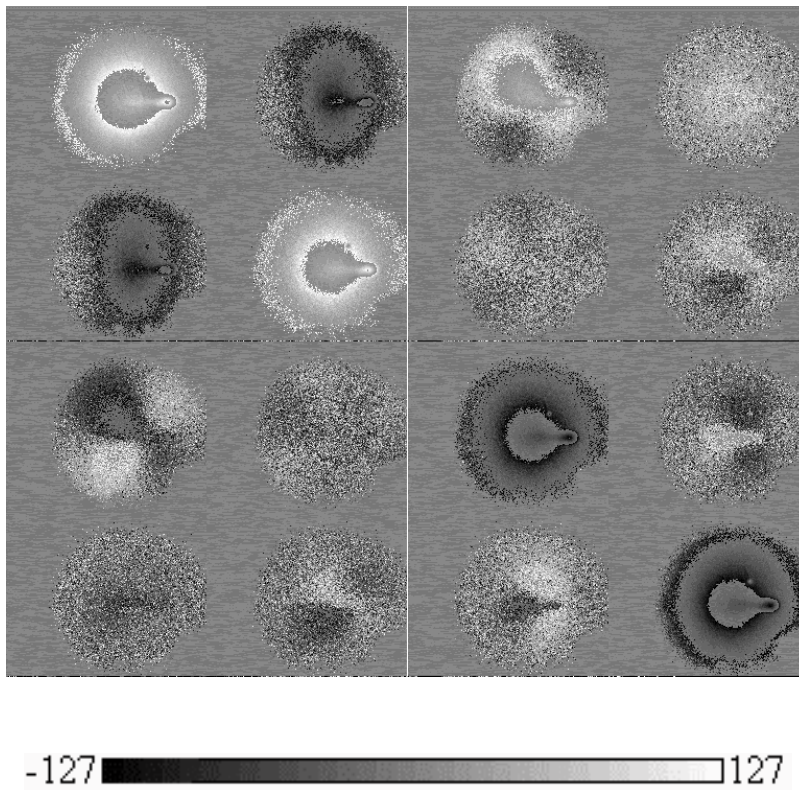
Fig. 8. Diffuse backscattering Mueller matrix components corresponding to a suspension of randomly distributed silica spheres (diameter 1500 nm) with $\mu_s^{'} = 0.32\ cm^{-1}$. The gray scale bar is adjusted so that black corresponds to negative and white represents positive values of the matrix component. Gray color means "no light" or component change by an order of magnitude. Gate delay time is 650 ps.
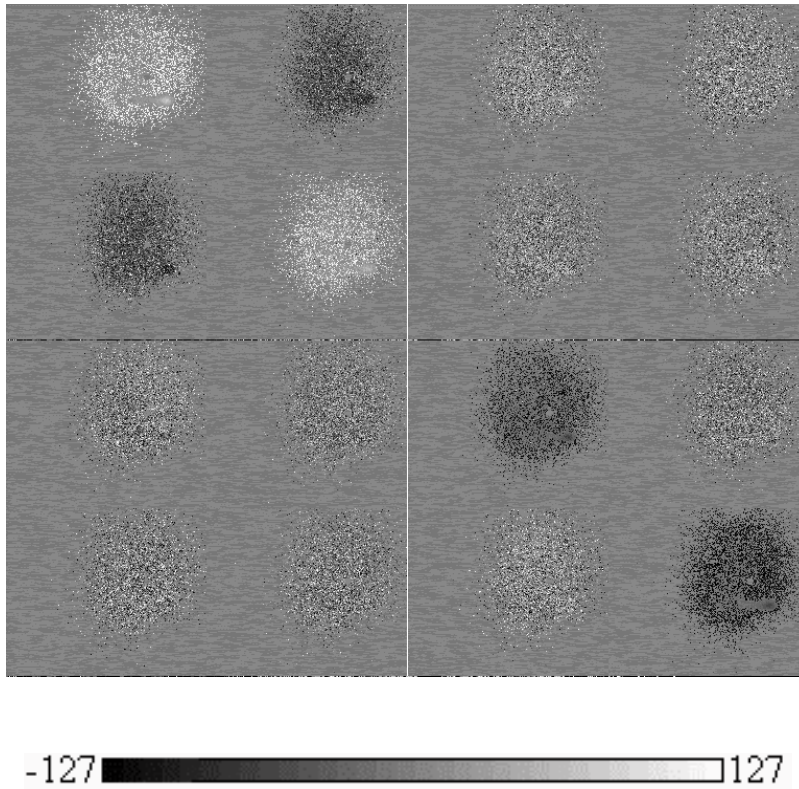
Fig. 9. Diffuse backscattering Mueller matrix components corresponding to a suspension of randomly distributed silica spheres (diameter 1500 nm) with $\mu_s^{'} = 0.32\ cm^{-1}$. The gray scale bar is adjusted so that black corresponds to negative and white represents positive values of the matrix component. Gray color means "no light" or component change by an order of magnitude. Gate delay time is 950 ps.
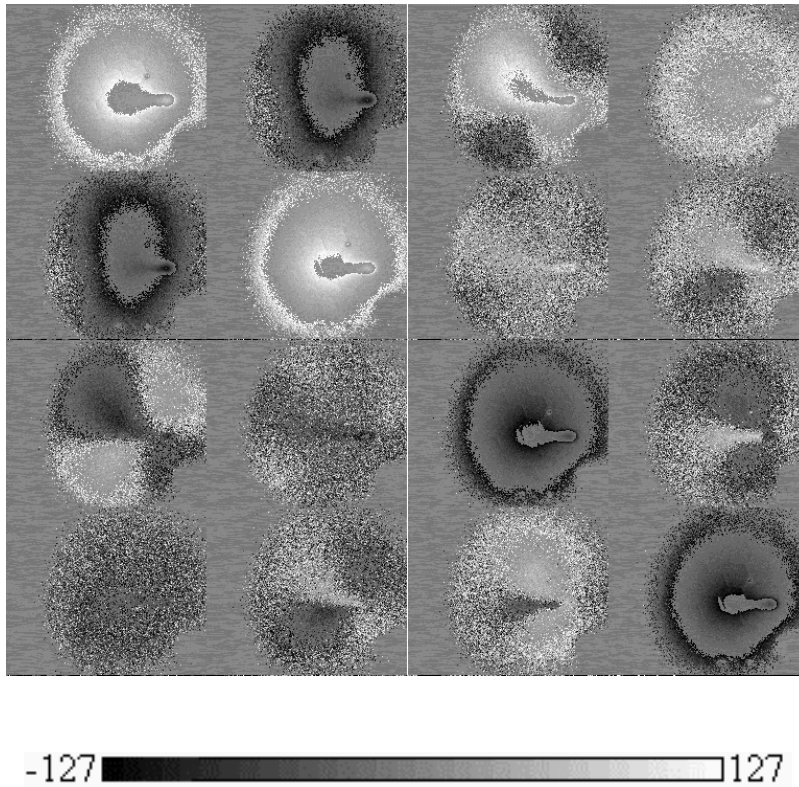
Fig. 10. Diffuse backscattering Mueller matrix components corresponding to a suspension of randomly distributed silica spheres (diameter 1500 nm) with $\mu_s' = 0.32 \; cm^{-1}$. The gray scale bar is adjusted so that black corresponds to negative and white represents positive values of the matrix component. Gray color means "no light" or component change by an order of magnitude. Time integrated matrix (integration for 31 time-steps).

As seen from the Figures 3-7 and 8-10, the polarization patterns follow the time evolution of the backscattering Mueller matrix. Therefore, by analyzing the corresponding series of the polarization patterns one can trace scattering events of different order. Specifically, the data analysis suggests several interesting observations regarding the general properties of the backscattering Mueller matrix. First, the magnitude of the off-diagonal components of the backscattering Mueller matrix is significantly smaller than the magnitude of the diagonal components. In terms of the average value of the amplitude of the spatial patterns, the 16 components of the Mueller matrix for each time step can be sorted in decreasing order of the magnitude of the pattern amplitude: 1) diagonal components, 2) M_{01} and M_{10}, 3) M_{02}, M_{20} and M_{12}, M_{21}, 4) components of the last row and the last column (excluding M_{33}). This tendency observed in our time-resolved data correlates well with earlier steady-state measurements on systems of similar size spheres [8], which showed a dependence of the magnitude of the components of the last row and last column on the particle size. The magnitude of the fourth group components (except M_{33}) is at the level of experimental errors for the 200 nm particles. Therefore, the symmetry relations for this group can only be assessed on experimental data for 1500-nm particles.

In the present experiments, we were able to trace the time evolution of the polarization patterns and to verify that the existing magnitude distributions are preserved in time. The magnitude and the sign of most of the spatial extent of the matrix components for the first and second groups closely resemble the form of the Mueller matrix for the case of single scattering from spheres [11]. Therefore, we conclude that for the optical densities used in our experiments, the Mueller matrix is mainly due to single backscattering processes. In other words, the weaker components from the third and fourth group mainly reflect features corresponding to multiple scattering processes. By comparing subsequent patterns in the time series, it can be seen that multiple scattering starts almost simultaneously with the single scattering process (Fig. 3) but it decays faster in time (Fig. 6, 9).

The next important observation is that the experimental results clearly display several symmetry properties of certain matrix components. Specifically, M_{01} and M_{10} components are equal. The components M_{02}, M_{20} and M_{12}, M_{21} are equal but have opposite signs. These symmetry relations hold throughout the entire time series, and are observed for all studied particle size and concentrations. The components M_{13}, M_{31} are equal while the components M_{23}, M_{32} and M_{03}, M_{30} are equal but have opposite signs (Fig. 8). The time-integrated backscattering Mueller matrix (Fig. 7, 10) holds the same symmetry relations as the time-resolved ones. Our experimental data clearly show that the Mueller matrix is not fully symmetric as stated in Ref. [8]. On the other hand, our results appear to be similar with those presented in Ref. [10] except for M_{03} and M_{30} which have significantly weaker magnitude.

By comparing the time-resolved (Fig. 4, 5) with the time-integrated (Fig. 7) matrices, one can identify the unique features of the Mueller matrix in time and spatial domains, which are otherwise hidden. Specifically, a part of the pixels in the patterns corresponding to M_{11}, M_{22}, M_{01} and M_{10} components exhibit a time-dependent behaviour, resulting in reversible changing of the sign of these components from positive to negative and vice versa. We relate these features with scattering events of higher order, which occur during the time of observation. As seen in the data, the contribution of higher-order scattering events becomes comparable with that of single scattering after a specific time delay.

5. Conclusion

Using a novel experimental capability, we performed the most comprehensive measurements of the time-resolved and spatially-resolved Mueller matrices corresponding to light diffusely backscattered from highly scattering media.

Each individual Muller matrix in the time series, as well as the resulting integrated steady-state Mueller matrix can be analyzed in terms of the amplitude value and the sign of the corresponding patterns. In our experiments, the scattering regime was adjusted to be at the incipient transition between single and multiple scattering. From an experimental standpoint this regime is most challenging because of the short time scales; on the other hand, it is rich in information content because the low-order scattering events are responsible for non-trivial polarization features. Our results demonstrate that the pairs of the off-diagonal components satisfy several symmetry relations: such as $M_{10} = M_{01}$, $M_{20} = -M_{02}$, $M_{21} = -M_{12}$, $M_{30} = -M_{03}$, $M_{31} = M_{13}$, $M_{32} = -M_{23}$. The experimental data clearly indicates that the pixels in the patterns of M_{11}, M_{22}, M_{01} and M_{10} components change sign during the life-time of the backscattering Mueller matrix, which presumably is associated with the dominating scattering events of higher order.

Temporally- and spatially-resolved measurements provide detailed information about the changes in the magnitude and sign of Mueller matrix components. This should offer more insight into early depolarization process in backscattering geometry and could lead to novel procedures for characterizing scattering phenomena. In addition, the time evolution of the symmetries between elements of the Mueller matrix could find applications in remote sensing and biomedical optics.

Acknowledgments